SIMULATION OF SEMICONDUCTOR DEVICES AND PROCESSES Vol. 3
Edited by G. Baccarani, M. Rudan - Bologna (Italy) September 26-28, 1988 - Tecnoprint

APPLICATION OF LOCAL NEUMANN ERROR CRITERIA FOR REMESHING IN DOPANT DIFFUSION PROBLEMS

R. Ismail and G. Amaratunga

Department of Engineering,
University of Cambridge,
Cambridge CB2 1PZ, U.K.

Summary

The finite element method is used more efficiently by applying a remeshing technique. The criteria for remeshing is based on an *a posteriori* error estimator. Both global and local error indicators are investigated. It is found that although the local error values are larger than the global error, it can locate where the maximum errors are in the finite element mesh. Its main advantage over global error evaluation is that it requires less CPU time to compute and thus is more suited for adaptive meshing applications in two dimensions. Results obtained when simulating a typical 2 dimensional MOS source/drain diffusion indicate a substantial reduction in runtime as compared to a solution using a static mesh.

1. Introduction

The numerical techniques for simulating dopant diffusion in silicon are well established. The current trend of research in this field is more towards improving the accuracy of existing physical models [1] as well as to model new processes. As the models become more sophisticated in order to achieve higher acccuracy, the CPU time required for 2D simulation is expected to increase substantially. Efforts have therefore to be made in developing more efficient numerical algorithms to reduce computational time [2][3][4]. One of the more commonly used numerical techniques for simulating dopant diffusion is the finite element method. In this work it is proposed that this method be used more efficiently by applying a remeshing scheme. This is because the computational efficiency and accuracy of the finite element method is closely linked to its mesh topology. By implementing an adaptive meshing scheme, the number of nodes used and thus the amount of computation involved in a solution can be optimised. To implement such a scheme a reliable criteria is needed in order to identify areas of the finite element mesh where refinement is required and areas where the mesh can be further coarsened. Such a criteria is obtained in this work by computing error estimates derived from the finite element solution itself. This can only be calculated after a solution has been obtained and is therefore termed an *a posteriori* error estimator. Use of an error based criteria can also ensure a 'good' solution as refinements are implemented when the mesh is too coarse to adequately represent a given continuum.

Errors in the computed solution are examined both globally and locally. Local

error indicators are advatageous in terms of efficiency as they are calculated using computations which involve one or a few neighbouring elements at a time. However, to ascertain whether the local error estimator indicates correctly where the large errors are in a given solution, a comparison is made between the local and global error calculation for one dimensional simulations. Further evaluation of the local error estimator is carried out by implementing node removal and introduction based on each error estimator in turn. The results obtained are then compared to see whether they are consistent with each other. Once the viability of the local error criteria for remeshing has been validated, it is then extended to simulating a key proceesing step in 2 dimensions. The process step under investigation is the simulation of the doping profile in MOS source/drain regions after annealing. As devices continue to shrink so as to achieve faster switching times, the 2D effects of the impurity profiles become critical in determining device performance. The simulation of this particular step is thus carried out in 2D.

2. Finite element formulation of the diffusion equation

The nonlinear equation governing dopant diffusion in silicon during the annealing stage is

$$\frac{\partial C}{\partial t} = \nabla(D(C)\nabla C) \tag{1}$$

where C is the dopant concentration, $D(C)$ is the concentration dependent diffusion coefficient and t is time. The weighted residual formulation is then applied to (1) and in particular the widely used Galerkin method is chosen. Thus using Green's theorem to reduce the differential operator and assuming that the flow normal to the boundary is zero, we obtain the weak form of (1) in 2D as

$$\int_A \left[\frac{\partial w}{\partial x}\left(D(C)\frac{\partial C}{\partial x}\right) + \frac{\partial w}{\partial y}\left(D(C)\frac{\partial C}{\partial y}\right)\right] dA + \int_A w\frac{\partial C}{\partial t} dA = 0 \tag{2}$$

where w is a suitable weighting function and integration is taken over the area A of the continuum. The unknown function C is approximated throughout the domain as

$$C = \sum_{i=1}^{m} N_i C_i \tag{3}$$

in which m is the total number of nodes in the finite element mesh, N_i the global shape funtions and C_i the nodal values of C. By substituting (3) into (2) and since in the Galerkin process $w_i = N_i$ we obtain the system of ordinary differential equations

$$K_{ij}C_j + M_{ij}\frac{\partial C_j}{\partial t} = 0 \tag{4}$$

where

$$\begin{aligned} K_{ij} &= \sum_{j=1}^{m}\left[\int_A \frac{\partial N_i}{\partial x}\left(D(C)\frac{\partial N_j}{\partial x}\right) + \frac{\partial N_i}{\partial y}\left(D(C)\frac{\partial N_j}{\partial y}\right) dA\right] \\ M_{ij} &= \sum_{j=1}^{m}\int_A N_i N_j dA \end{aligned} \tag{5}$$

K and M are commonly known as the global stiffness and mass matrices respectively. In practice however, the global stiffness and mass matrices are not directly constructed

according to (5). Instead the expressions in (5) are used to establish the stiffness and mass matrices for each element seperately. These are then assembled to give the global expressions. The type of finite element used in this analysis is the triangle with linear variation in the unknown C. To remove the instability problem that is sometimes encountered, a lumped (or diagonal) mass matrix [5] is used for M_{ij} in (5).

The finite element method can again be applied to (4) to discretise the time domain. Using a two level time-stepping scheme which relates C_{n+1} to C_n and approximating the time derivatives by finite differences leads to

$$\left[K\theta + \frac{1}{\Delta t}M\right] C_{n+1} + \left[(1-\theta)K - \frac{1}{\Delta t}M\right] C_n = 0 \tag{6}$$

where Δt is the step size in time. The scheme parameter θ can be varied between 0 and 1 to produce any number of different schemes. However, for an unconditionally stable and oscillation free solution, a fully implicit scheme with $\theta = 1$ is used [6]. The resultant sparse global matrix is solved using a fast direct solver employing the frontal method. To account for the variation of the elemental diffusion coefficient over a time step, inner iteration is carried out within each Δt. Newton's method is used because of its faster rate of convergence.

3. Global and local error analysis

The approach taken here is to solve for the error function directly [7]. Consider again the two dimensional diffusion equation in (1). Assume that an estimate of the ideal solution C has been obtained using a second order basis function β and the approximate solution C_a is obtained using a first order basis function. Then the error ξ equals the difference between the exact solution and the approximate solution

$$\xi = C - C_a \tag{7}$$

Applying the finite element method described in the last section and substituting (7) into (4) we obtain

$$\sum_{j=1}^{m}\left[\int_A \nabla\beta_i D(C_a+\xi)\nabla\beta_j dA\right](C_a+\xi)_j + \sum_{j=1}^{m}\left[\int_A \beta_i\beta_j dA\right]\frac{\partial(C_a+\xi)_j}{\partial t} = 0 \tag{8}$$

$$i = 1,2,3,\ldots m$$

Now (8) has to be solved iteratively if we take the diffusivity to be $D(C_a+\xi)$. The value of ξ thus obtained will be the error due to the spatial discretisation, and the effect of this error on the nonlinear diffusion coefficient. However, if we are only interested in the error due to the coarseness of the mesh, we can assume $D(C_a+\xi)$ to be $D(C_a)$. Hence writing in a more concise form

$$\tilde{K}_{ij}(C_a+\xi)_j + \tilde{M}_{ij}\frac{\partial(C_a+\xi)_j}{\partial t} = 0 \tag{9}$$

where $\tilde{K}$ and $\tilde{M}$ are the second order stifness and mass matrices

$$\tilde{K}_{ij} = \sum_{j=1}^{m}\left[\int_A \nabla\beta_i D(C_a)\nabla\beta_j dA\right]$$

$$\tilde{M}_{ij} = \sum_{j=1}^{m}\left[\int_A \beta_i\beta_j dA\right] \tag{10}$$

$$i = 1,2,3\ldots m$$

Using a fully implicit time stepping scheme we obtain the matrix

$$-\left[\tilde{K}_{ij}+\frac{\tilde{M}_{ij}}{\Delta t}\right]\left[\xi_j^{n+1}\right]=\left[\tilde{K}_{ij}+\frac{\tilde{M}_{ij}}{\Delta t}\right]\left[C_{aj}^{n+1}\right]-\left[\frac{\tilde{M}_{ij}}{\Delta t}\right]\left[C_{aj}^{n}+\xi_j^{n}\right] \tag{11}$$

The use of the full set of piecewise continuous quadratic polynomials for the error ξ above requires the assembly and solution of a 6 by 6 matrix equation for each of the elements in the finite element mesh. Obviously this requires a greater computation time than for the calculation of the original solution and becomes prohibitively expensive as the number of elements increase. An alternative approach as proposed by Bank and Weiser [8], is based on solving a local Neumann problem in each element of the finite element mesh. If we apply equation (9) to a single finite element E we have

$$\tilde{K}_{ij}^{E}(C_a+\xi)_j+\tilde{M}_{ij}^{E}\frac{\partial(C_a+\xi)_j}{\partial t}-\int_S \beta_i D(C_a)\frac{\partial C}{\partial N_E}dS=0 \tag{12}$$

For a given value of C_{aj} we can compute every quantity in (12) except $\frac{\partial C}{\partial N_E}$ on the boundary of E. Suppose E shares side s with a neighbouring element E′ as shown in Fig. 1 below;

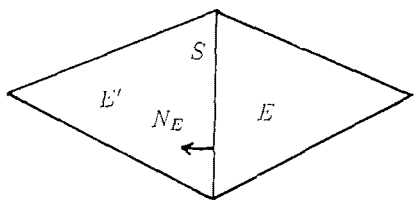

Fig. 1 *Two elements sharing an edge s*

Considering the edge s, a possible approximation to $\frac{\partial C}{\partial N_E}$ is the average value of $\frac{\partial C_a}{\partial N_E}$ on E and E′, where N_E is the outward normal from E [9]. Since

$$N_E=-N_{E'}$$

we define the approximation

$$\left[\frac{\partial C_a}{\partial N_E}\right]_J=\begin{cases}\frac{1}{2}\left(\frac{\partial C_a}{\partial N_E}-\frac{\partial C_a}{\partial N_{E'}}\right), & \text{s not in } \partial\Omega\\ 0, & \text{s in } \partial\Omega\end{cases} \tag{13}$$

where $\partial\Omega$ is the boundary of the bounded domain of interest. Hence the resulting approximation to (12) is

$$\tilde{K}_{ij}^{E}(C_a+\xi)_j+\tilde{M}_{ij}^{E}\frac{\partial(C_a+\xi)_j}{\partial t}-\int_S \beta_i D(C_a)\left[\frac{\partial C_a}{\partial N_E}\right]_J^{S_i}dS=0 \tag{14}$$

where the value of $\left[\frac{\partial C_a}{\partial N_E}\right]_J^{Si}$ depends on which side S_i of the triangular element the integral is taken. Again using a fully implicit time stepping scheme, the expression for a single element is

$$\begin{aligned}-\left[\tilde{K}_{ij}^{E}+\frac{\tilde{M}_{ij}^{E}}{\Delta t}\right]\left[\xi_j^{n+1}\right]=&\left[\tilde{K}_{ij}^{E}+\frac{\tilde{M}_{ij}^{E}}{\Delta t}\right]\left[C_{aj}^{n+1}\right]-\left[\frac{\tilde{M}_{ij}^{E}}{\Delta t}\right]\left[C_{aj}^{n}+\xi_j^{n}\right]\\&-\int_S \beta_i D(C_a)\left[\frac{\partial C_a}{\partial N_E}\right]_J^{S_i}dS\end{aligned} \tag{15}$$

The above analysis leads directly to an error indicator defined element by element and is more efficient because it is derived from local computations.

4. Comparison between global and local error

Both the above error formulations were implemented on the pseudo 2D mesh shown in Fig. 2 below;

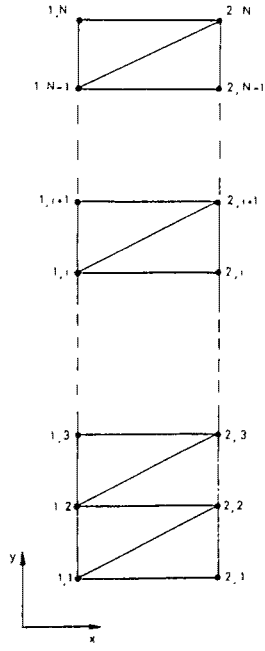

Fig. 2 *Finite element mesh used in the 1D simulations*

Fig. 3a(i) shows the initial profile to be simulated, which is arsenic implanted with a dose of 5E15 atoms/cm^2 at 75 keV. Fig. 3b(i) shows the diffusion profile after 20 minutes of annealing at 1000°C with a 30 seconds time step. The points on the profile indicate nodal distribution and the square symbols on the profile of Fig. 3b(i) are experimental data obtained using SIMS. Fig. 3a(ii) and Fig. 3b(ii) shows the corresponding global error profiles and Fig. 3a(iii) and Fig. 3b(iii) are the profiles for the local error. As can be seen the maximum global and local errors occur at the steep front of the diffusion profiles and the values of the global error are between 9 and 15 per cent. We can see that there is a good agreement between the simulated diffusion and the experimental data. Thus it seems that a global error of about 15 per cent or below together with a 30 seconds time step is acceptable for obtaining a good solution. This error value will be use later as a limit over which an element should be refined. As can be seen, the local error estimator agrees well with the global error estimator as to where the maximum error on the diffusion profiles are. However, the local error values are generally about 3 times larger than the global error values. It was also found that it took about 30 per cent more CPU time to compute the global error distribution as compared to the local error distribution for this particular test problem.

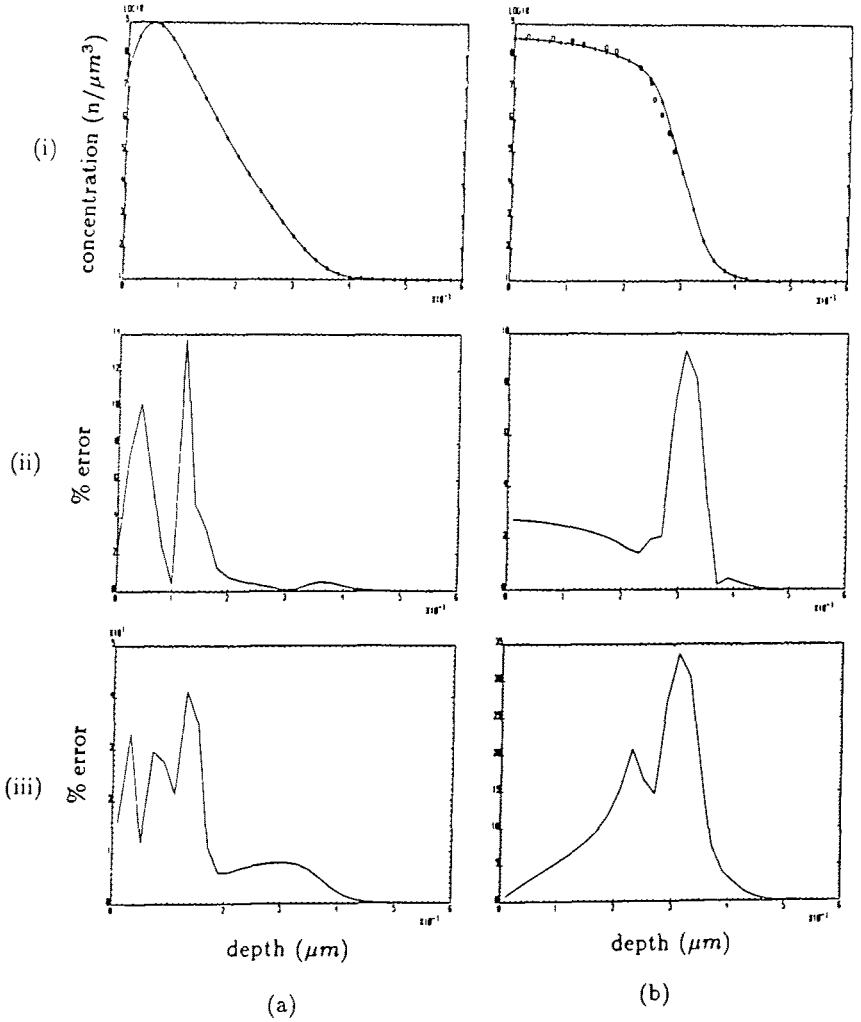

Fig. 3

Comparison between global and local error profiles.

(i)a,b *Initial and diffused concentration profiles for arsenic (5E15n/cm², 75 keV) implant.*

(ii)a,b *Global error profiles.*

(iii)a,b *Local error profiles.*

5. Global versus local error criteria for remeshing

Using the same form of mesh shown in Fig. 2, the remeshing based on the above error indicators are compared. To begin with, a very coarse initial mesh which is just sufficient to describe the geometry of the implant profile is chosen. This profile is show in Fig. 4(a) for an arsenic implant with a dose of 5E15 atoms/cm^2 and energy of 75 keV to be annealed at 1000°C for 20 minutes. The total number of nodes for this initial profile is 18. After the first timestep of 30 seconds the global error profile is shown in Fig. 4(b) and the local error profile in Fig. 4(c). From the last section a suitable criteria for remeshing based on the global error which can give a good solution was found to be 15 per cent or less. Nodes are then introduced if the global error exceeds 12 per cent and nodes are eliminated from the mesh if the global error is less than 3 per cent. On the other hand for remeshing based on the local error criteria, nodes are introduced if the error values exceed 30 per cent and are eliminated if it is less than 10 per cent since their values are generally three times larger than the global error. The new initial mesh after remeshing using the global error criteria is shown in Fig. 5(a). The total number of nodes is now 24 i.e. 6 new nodes have been introduced. Fig. 5(b) shows the global error profiled obtained after a solution using this new mesh. It can be seen that the introduction of the new nodes resulted in the error being reduced to the desired level. When the local error criteria is used, 7 new nodes are introduced into the initial mesh. The positions at which the new nodes are introduced are in good agreement to those at which nodes are introduced using the global error criteria, as can be seen on comparing Figs. 5(c) and Figs. 5(a). Fig. 5(d) also shows that as a result of the remeshing, the error has been reduced to the desired local value. Error evaluation and remeshing is then carried out at each time step. The diffusion profiles and nodal positions after 20 minutes of difusion are shown in Figs. 6 for both remeshing schemes. As can be seen a good agreement in terms of nodal distribution is obtain between the two profiles. Thus the remeshing scheme based on the local error criteria does produce results which are consistent with those obtained using remeshing based on the global error criteria.

Further experiments showed that whilst the introduction of new nodes can reduce the maximum error to about 20 per cent of its original value, halving the timestep reduces the maximum error by only 5 per cent. This suggests that the error is due more to the meshing than the time stepping. However, by doubling the time step to 60 seconds, it was found that not only did the maximum global error increase substantially but that its position had also been altered. Clearly the increase in the maximum error was in this case due to the time step. Thus it seems that a time step of 30 seconds is a suitable choice for obtaining correct error profile, which is mainly due to the spatial discretisation. It should however be noted that in general some experiments have to done to determine the time step as it will vary depending on the diffusion conditions such as temperature, dose and dopant type.

6. Application of local Neumann error criteria for adaptive meshing in 2D

The remeshing based on the local error criteria is now extended to a two dimensional problem. The initial mesh is designed such that equilateral triangles are used wherever possible. The error resulting from the first time step is used to refine the original mesh by actually doing implant value calculations for each new node that is introduced. Delaunay triangulation is used to form the mesh after each refinement. Refinement for any element is done by adding new nodes at the midsides of each side of a triangular element. This ensures the generation of further equilateral triangles and reduces the possibility of generating obtuse angled triangles in the mesh. The refine-

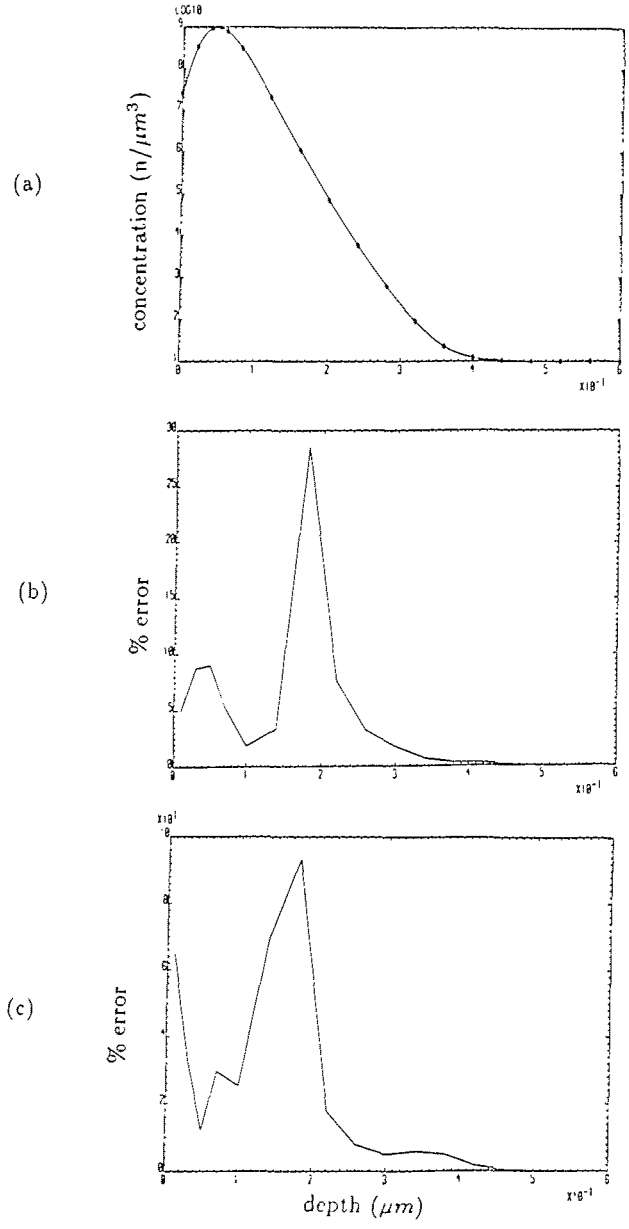

Fig. 4
Initial concentration profile showing nodal distribution and error profiles before remeshing.
(a) *Initial implant profile for a 75keV, 5E15/cm² As implant.*
(b) *Global error profile.*
(c) *Local error profile.*

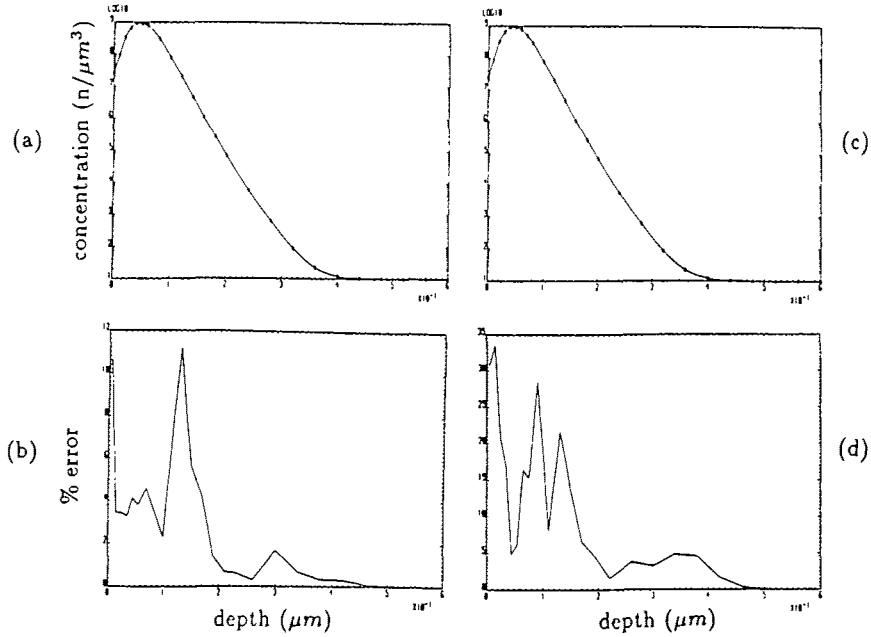

Fig. 5

Initial concentration profiles of Fig. 4(a) indicating nodal positions after remeshing and their corresponding error profiles.
(a) *Concentration profile after remeshing based on global error.*
(b) *Corresponding global error profile.*
(c) *Concentration profile after remeshing based on local error.*
(d) *Corresponding local error profile.*

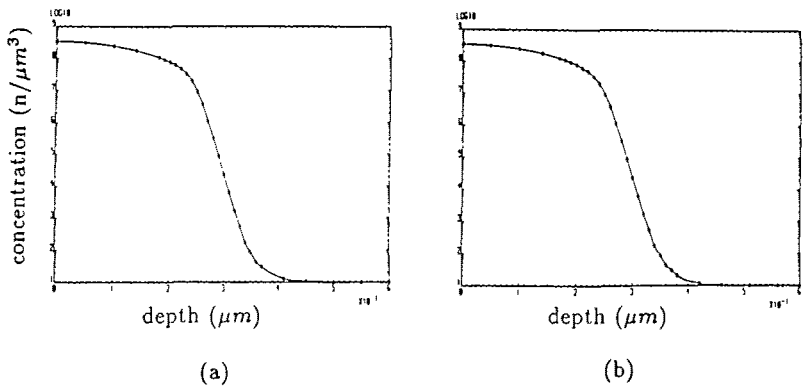

Fig. 6

Diffusion profiles indicating nodal position after 20 minutes diffusion at 1000°C;
(a) *remeshing based on global error profile.*
(b) *remeshing based on local error profile.*

ments are applied to a basic core mesh which is preserved throughout the diffusion. This enables the core mesh to be refined while removing nodes from the previous time step which are not required for the current time step. The core mesh must be such that it has sufficient nodes for interpolation of values for new nodes over the entire diffusion time. This can be determined at the start by examining the physical diffusion parameters and ensuring that the error is reduced to the required level by a single refinement after the first time step. Figs. 7 and Figs. 8 shows the evolution of the mesh and concentration profile when simulating a 5E15 atoms/cm^2, 75keV arsenic implant diffusion at 1000°C for 20 minutes. It can be seen that the mesh refinement follows the steep front of the concentration profile where the maximum errors are expected. This result was compared to a solution using a static mesh in which the entire core mesh was refined. The profile after 20 minutes diffusion was the same but it took 3 times longer to simulate.

7. Conclusion

A remeshing technique based on *a posteriori* error criteria has been presented. Investigation into global and local error showed that the local error estimator can be used as a criteria for remeshing but with a value about 3 times larger than the global error estimator. The remeshing scheme based on local Neumann error criteria has been successfully implemented for simulating two dimensional diffusion of MOS source/drain regions and on average resulted in a 65 per cent reduction in CPU times as compared with solutions based on a static mesh.

References

1. H.R. Yeager and R.W. Dutton, " An approach to solving multiparticle diffusion exhibiting nonlinear stiff coupling", *IEEE transactions on computer-aided design of integrated circuits and systems*, vol. CAD-4, No. 4, p.408, October 1985.
2. G.A.J. Amaratunga and R. Ismail, "A quasi-linear formulation with a simple remeshing scheme for the finite element based simulation of dopant diffusion in silicon", *IEE Proc. on solid-state and electron devices*, vol. 133, Part 1, December 1986.
3. P. Pichler et al, "Simulation of critical IC fabrication steps", *Trans. IEEE*, ED-32, p.384, October 1985.
4. R. Biswas, "Parallel computation methods for simulating dopant diffusion in silicon", *Cambridge Engineering Department first year research report*, April 1987.
5. I. Fried and D.S. Melkus, "Finite element mass matrix lumping by numerical integration with no convergence rate loss", *Int. J. Solids Struct.*, 11, 461-5, 1975.
6. O.C. Zienkiewicz and K. Morgan, 'Finite elements and approximation', Wiley, 1980.
7. Z.J. Zendes and D.N. Shenton, "Adaptive mesh refinement in the finite element computation of magnetic fields", *IEEE transaction on magnetics*, Vol. MAG 21, No. 5, September 1985.
8. R.E. Bank and A. Weiser, "Some *a posteriori* error estimators for elliptic partial differential equations", *Mathematics of Computation*, vol. 44, No. 170, April 1985, pp. 283-301.
9. A. Weiser, "Local-mesh, local-order, adaptive finite element methods with *a posteriori* error estimators for elliptic partial differential equations", Technical report 213, Computer science department, Yale University, 1981.

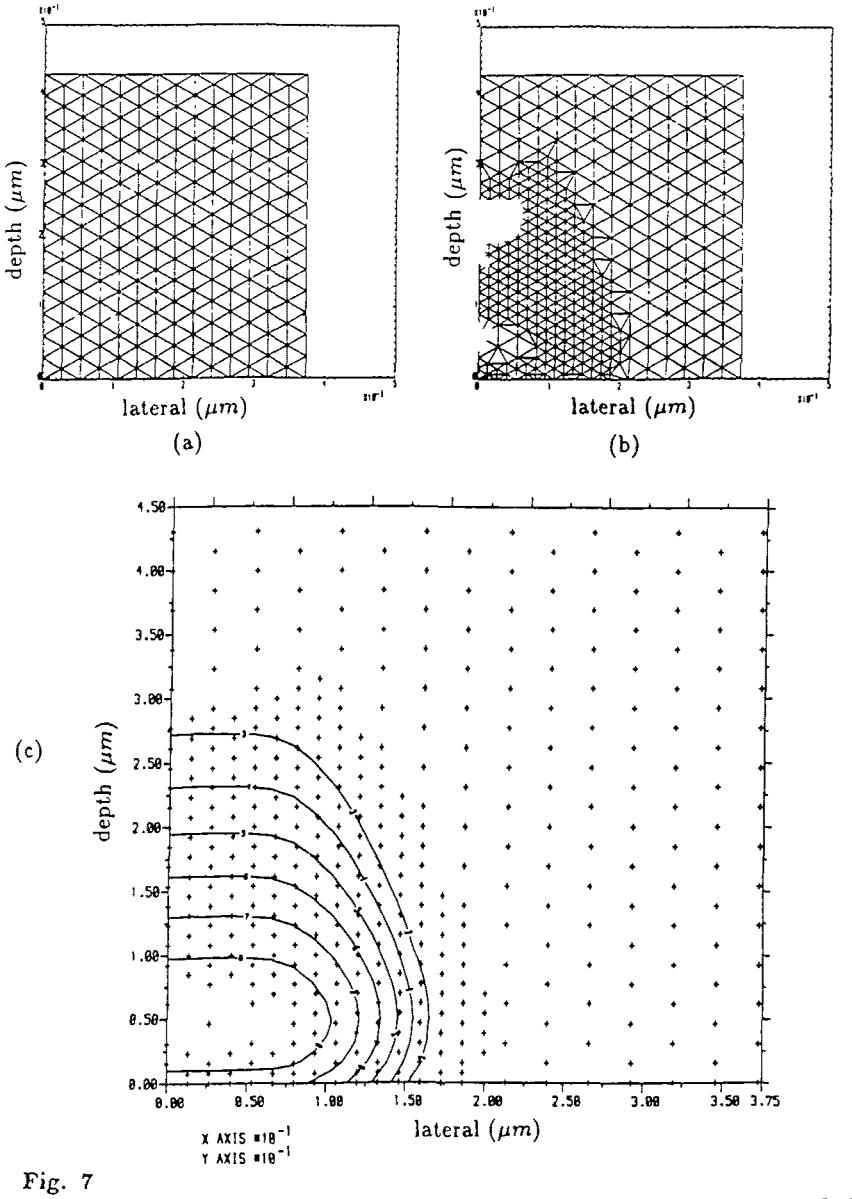

Fig. 7

Two dimensional remeshing results based on local error criteria for a 75 keV, 5E15 n/cm^2 as implant to be annealed at 1000°C.

(a) *Initial core mesh which is preserved throughout the diffusion.*

(b) *Initial refinement for the implant profile.*

(c) *Initial implant profile. Contours log10 values of concentration ranging from 1E3(deepest) to 1E8 (nearest surface) in n/μ^3. Crosses indicate nodal positions.*

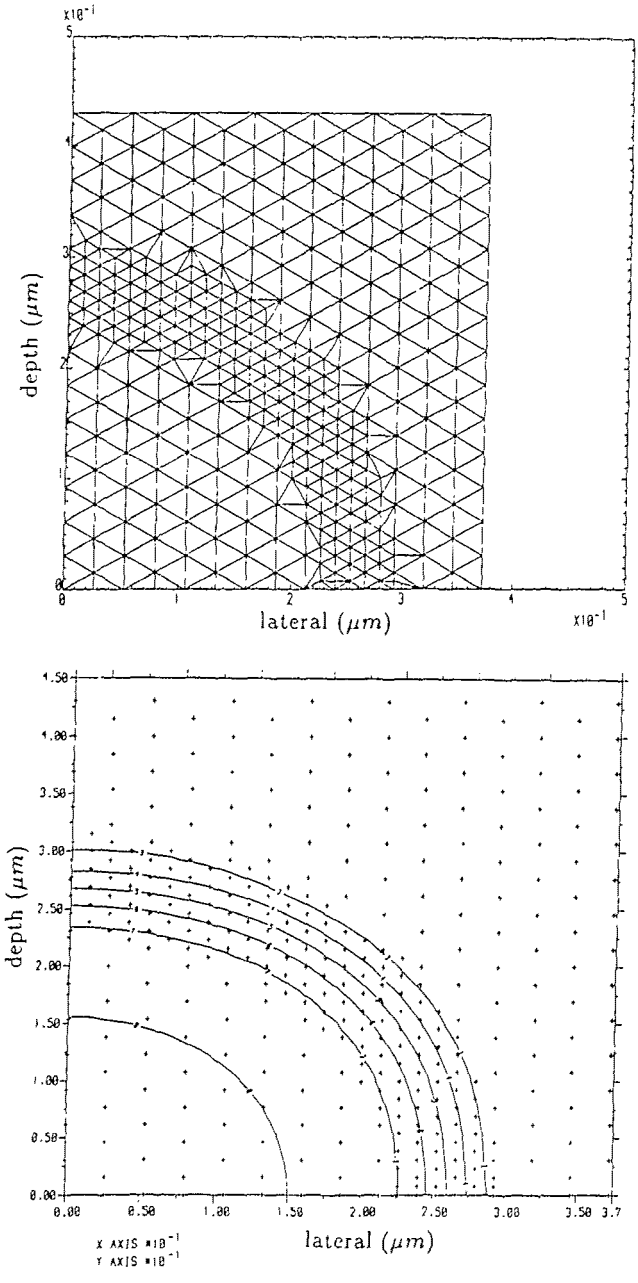

Fig. 8

Mesh and concentration profiles after 20 minutes diffusion. Contour values as in Fig. 7(c)